Anton Marcinčin,
Konštantín Marcinčin,
Marcela Hricová,
Anna Ujhelyiová,
***Jaroslaw Janicki,**
***Czeslaw Ślusarczyk**

Department of Fibers and Textile Chemistry, Faculty of Chemical and Food Technology,
Slovak University of Technology in Bratislava,
Radlinskeho 9, 812 37 Bratislava, Slovak Republic
E-mail: marcela.hricova@stuba.sk

***Institute of Textile Engineering**
and Polymer Materials,
University of Bielsko-Biala,
Willowa 2, 43 309 Bielsko-Biala, Poland

Structure, Thermal and Mechanical Properties of PP/Organoclay Composite Fibres

Abstract

In this paper, the effect of the uniaxial deformation of PP/organoclay composite fibers in spinning and drawing on their supermolecular structure as well as thermal and mechanical properties is presented. Commercial organoclays Cloisite C15A and Cloisite C30B, both based on montmorillonite (MMT), were used as inorganic fillers in the experimental work. The supermolecular structure of fibers was investigated by DSC analysis and X-ray diffraction (WAXS). The DSC measurements were carried out using the conventional method (CM) and constant length method (CLM), in which fibers of constant length were assured during measurement. The average orientation of fibers was evaluated by the sonic velocity method. The intercalation of polypropylene in interlayer galleries of the organoclay was evaluated by the SAXS method. The tenacity and Young's modulus of composite fibers were evaluated and discussed with regard to their thermal properties and supermolecular structure, as well as the intercalation and exfoliation of the (nano)filler in the polymer matrix.

Key words: *nanocomposites, fibers, SAXS, thermal properties, mechanical properties.*

Introduction

The incorporation of organoclay into semicrystalline polymers affects their crystalline properties, such as crystallisation kinetics, crystal structures and the total crystallinity [1, 2]. The layered silicates in the polypropylene (PP) matrix behave as effective heterogeneous nucleating agents, enhancing the crystallization rate [2] and, at the same time, decreasing the spherulite size and perfection of the crystals as well as shifting the cooling crystallization temperature to higher values [3]. Besides this the silicate nanoplatelets affect the shear flow induced crystallisation and retardancy of the crystallisation kinetic of the matrix during the quiescent crystallisation of PP/montmorillonite (MMT) composites [4-6]. The preferential orientation of PP lamellae perpendicular to the surface of the organoclay layers was found for PP/talc composite via TEM observation [7]. The lamellar orientation on the clay layers was ascribed to nucleation and crystallisation at the surface of the silicate platelets. Moreover the asymmetric morphology of crystals was observed in PP/organoclay nanocomposites at higher temperature [8] and at shear induced formation of the oriented threadlike crystallites [1].

The high oriented structure elements of fibres are considered in the development of the high tenacity and high modulus of fibres. The advantages of most semicrystalline polymers are their ability to self reinforce via the formation of a fibrillar structure during deformation at a relatively high temperature [9 - 11].

Simultaneously with the development of highly oriented polymers, suitable methods for the investigation of an oriented polymer structure were developed or modified [12]. Particularly Raman spectroscopy and X-ray diffraction enable the investigation of the molecular and crystal deformation of composite fibres in detail [13]. A special method of DSC analysis of fibres, known as the 'constrain method' or method of 'the constant length of fibres' (DSC-CLM), has been described in several papers. This DSC method is particularly suitable for evaluation of oriented structure elements of composite fibres [14, 15].

In our previous papers the effect of organoclay on the mechanical properties of PP fibres was studied [16, 17]. Surprisingly the orientation of polymer suppresses the effect of organoclay on the tenacity and Young's modulus of composite fibres, which is characteristic for isotropic polymer. The positive effect of organoclay on the mechanical properties of fibres was found for a very low concentration of solid particles only. In this case the contribution of nanoparticles as hard segments on mechanical properties is negligible. Thus the enhancement of the mechanical properties of composite fibres is affected indirectly by the suitable structure obtained at the maximal orientation (maximal draw ratio) of fibres. Some convenient methods were used for characterisation of the structure and morphology of PP composite fibres in our experimental work to explain their mechanical properties. The results are presented in this paper.

Experimental

Material used

Polymers

Two commercially available types of PP were used in the experimental work: polypropylene HPF (PP HP) with a melt flow index (MFI) of 8.0 g/10 min, in powder form and fibre-grade polypropylene TG 920 (PP) with an MFI of 10.5 g/10 min. Both polypropylenes were produced by Slovnaft a.s., Bratislava, Slovak Republic.

Fillers

The two kinds of organoclays (OC) used in this work were Cloisite 15A (C15A) and Cloisite 30B (C30B), both produced by Southern Clay Product, Inc, Gonzales, TX 78629, USA. C15A is a montmorillonite ion exchanged with dimethyl dihydrogenated tallow quartery ammonium ions. C30B is montmorillonite treated with methyl tallow bis-2-hydroxyl quartery ammonium ions.

Compatibilisers

Two different non-reactive compatibilisers-dispersants were used for preparation of the concentrated dispersion of organoclay in the PP HP. Commercially available Slovacid 44P (S44P), based on the ester of stearic acid and polypropylene glycol, produced by Sasol GmbH, Brunsbuettel, Germany, and Tegopren 6875 (TEG) based on poly (alkylsi-

loxane), produced by Degussa Co., Düsseldorf, Germany.

Preparation of polypropylene/ organoclay composite fibre

Preparation of concentrated dispersion of solid particles in PP

The PP HP, organoclay and compatibiliser were mixed in a high rpm mixer for a defined time. The powder mixture was melted and kneaded using a twin screw corotating extruder φ 28 mm. The temperatures of the extruder zones from the feedstock to the head were 80, 150, 220, 225, 225, 225 and 232 °C. The temperature of the extruded melt was 229 °C. The extruded produce was cooled and cut. The concentration of organoclay in the PP HP was 10.0 wt.% and the content of compatibiliser was 4.0 wt.%.

Melt mixing of concentrated organoclay dispersion with PP using a one screw extruder and consequential spinning of PP composite:

The chips of organoclay concentrate dispersion and PP were mixed and spun using a single screw extruder φ 30 mm and spinneret with 40 orifices. The spinning temperature was 280 °C, metering of melt 30 g/min, spinning speed 360 m/min and the fineness of spun fibres (drawn ratio 1:1, λ_1) was 840 dtex. Fibres were drawn using a laboratory drawing machine at a draw ratio of 1:3 (λ_3) and at the maximum drawn ratio (λ_{max}), at a drawing temperature of 120 °C.

Methods used

DSC measurement

Measurements were performed using a Perkin Elmer DSC 7 in the temperature range 30 - 200 °C. The standard heating rate was 10 °C/min. The measurements were carried out using the conventional method (DSC-CM), in which cut fibres of 1 - 2 mm length were used, and constant length method (DSC-CLM), in which the constant length of fibres during measurement was assured. A constant length of fibres was achieved through the winding and fixation of fibres on a wire. The melting peak temperature T_m and melting enthalpy ΔH_m were evaluated.

X-ray scattering method

Wide-angle scattering (WAXS) method: The structure of fibres was evaluated by the wide-angle X-ray scattering method. The investigations were carried out using a Seifert X - ray diffractometer. On the basis of the WAXS patterns, parameters characterising the fibre structure were determined. The total crystallinity X_α and content of the mesophase X_m were calculated as a ratio of the area under the crystalline or mesophase peaks to the total area [18].

Small-angle scattering (SAXS) method

All SAXS patterns were recorded with an MBraun SWAX camera with the Kratky collimation system, equipped with a PSD 50 MBraun linear position sensitive detector. The X-ray tube was a conventional copper anode operated at 40 kV and 30 mA, controlled by a Philips PW 1830

X-ray generator. Cu Kα radiation was obtained by filtering with Ni and pulse height discrimination. The powders were measured at room temperature while being kept in a standard sample holder, sealed with aluminium foil.

Orientation of fibres

The average factor of orientation of fibres (f_α) was evaluated by sonic velocity measurements using a Dynamic Modulus Tester-PPM-5R.

Mechanical properties of the blend fibres: An Instron (model 3343) was used for measurement of the mechanical properties of fibres (according to ISO 2062:1993), evaluated from 15 measurements. The initial length of fibres was 25 cm and the time of deformation was about 20 sec.

■ Results and discussion

Thermal properties and supermolecular structure of fibres

The DSC-CM method provides a simple one-peak thermogram for undrawn fibres and a characteristic double-peak thermogram for the middle draw ratio of fibres (*Figure 1.a*).

The radically different shapes of melting endotherms were observed for PP fibres in dependence on the draw ratio using the DSC-CLM method. The endotherm peak is gradually shifted to a higher temperature when the draw ratio increases (*Figures 1.b* & *1.c*). The one-peak endotherm
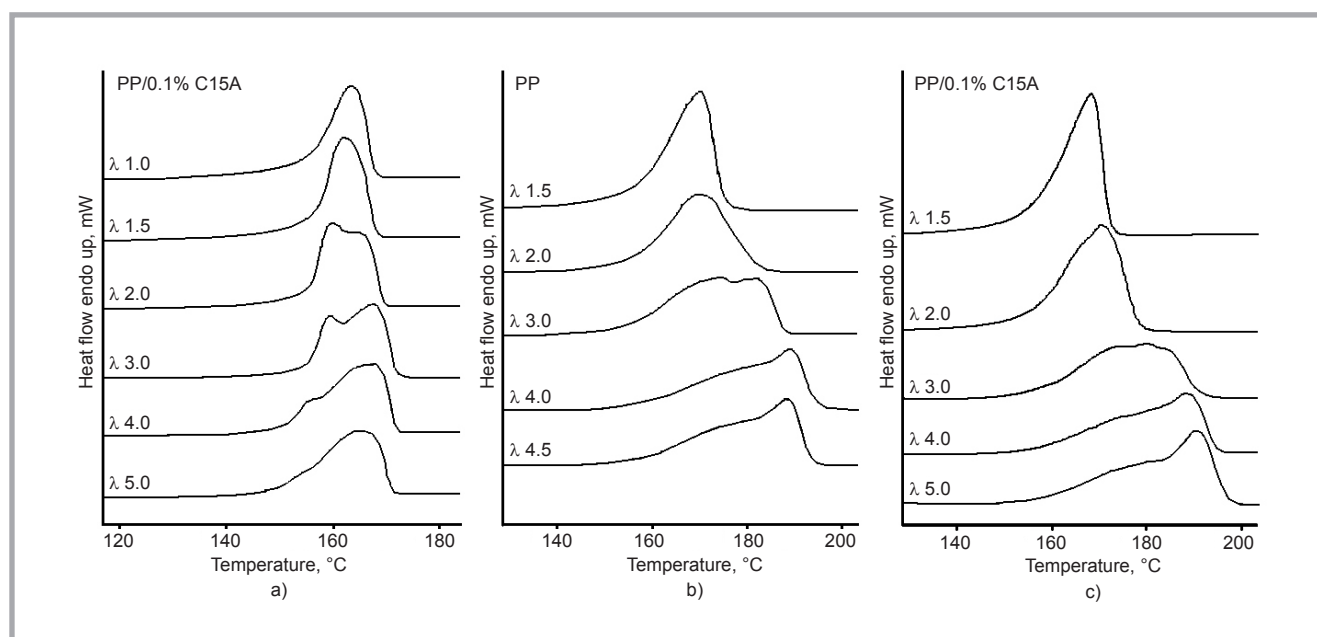

***Figure 1.** DSC-CM (a) and DSC-CLM (b, c) melting thermograms of PP and PP/0.1%C15A composite fibres in dependence on draw ratio.*
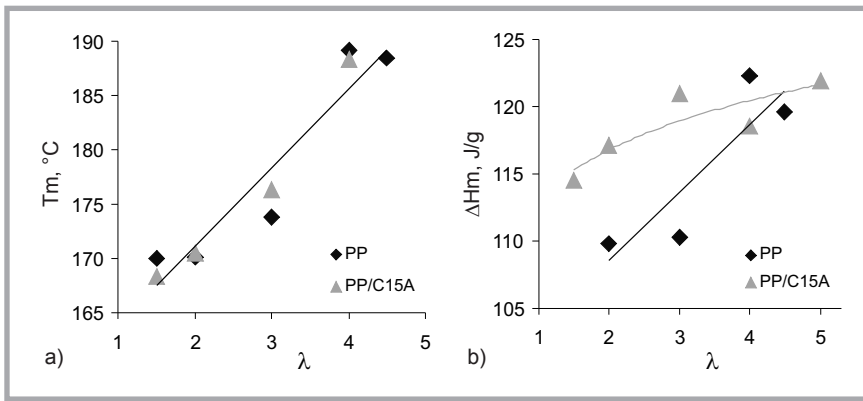
Figure 2. DSC-CLM melting temperature T_m (a) and melting enthalpy ΔH_m (b) versus draw ratio of PP composite fibres.
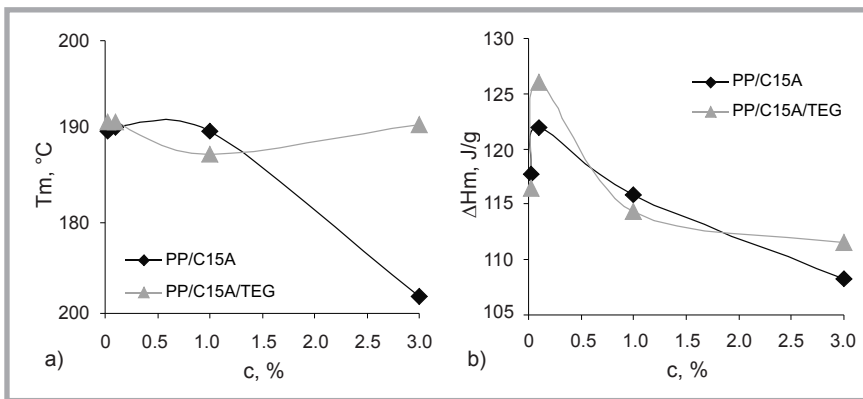

Figure 3. DSC-CLM melting temperatures Tm (a) and melting enthalpy ΔHm (b) versus concentration of organoclay in the PP fibres

Table 1. Results of WAXS measurements of PP/organoclay composite fibres.

Sample	Draw ratio, λ	Total crystallinity, x_C	Fraction of α form x_α	Fraction of mesophase, x_m	Sizes of crystallites of α form, $D_{(110)}$, nm	Sizes of mesophase crystallites, nm
PP	3.0	0.621	0.338	0.283	6.5	3.4
PP	4.5	0.625	0.311	0.314	5.4	3.1
PP/1.0% C15A	1.0	0.620	0.272	0.348	8.4	3.3
PP/1.0% C15A	3.0	0.668	0.407	0.261	7.1	3.4
PP/0.02% C15A	5.0	0.714	0.338	0.376	6.2	2.7
PP/0.1% C15A	5.0	0.688	0.347	0.341	4.6	2.8
PP/1.0% C15A	4.5	0.627	0.311	0.316	7.0	3.1
PP/3.0% C15A	3.0	0.571	0.388	0.183	11.6	3.5
PP/1.0% C30B	3.0	0.616	0.409	0.207	7.7	3.7
PP/1.0% C30B	4.5	0.658	0.389	0.269	6.3	3.1
PP/1.0% C30B/TEG	3.0	0.636	0.396	0.240	6.6	3.8
PP/1.0% C30B/TEG	4.5	0.636	0.435	0.201	5.2	4.0

becomes wider with an increase in the draw ratio.

The melting temperature (T_m) and melting enthalpy ΔH_m for PP fibres and PP/C15A composite fibres increase proportionally with the draw ratio up to the maximum values (**Figure 2**). Generally the DSC-CLM method provides a higher melting enthalpy for PP/organoclay fibres (higher crystallinity) in contrast to

the DSC-CM method, particularly for a lower draw ratio.

The effect of organoclay concentration on melting temperatures T_m is illustrated in **Figure 3.a**. The melting temperature passes through a slight maximum at 0.02 - 0.1 wt% of organoclay and decreases at a higher concentration of nanoparticles. The decrease in the melting temperature of oriented fibres obtained

by the DSC CLM method is proportional to the decrease in orientation of the non-crystalline phase, with an approximately average orientation. A decrease in the melting temperature (DSC CLM method) does not depend on the orientation of the crystalline phase. The dependence of enthalpy (crystallinity) on organoclay concentration exceeds the clear maximum at 0.1 wt.% and practically does not change with the presence of a compatibiliser-dispersant (**Figure 3.b**).

WAXS and SAXS measurements

The total crystallinity of the oriented PP matrix of fibres consists of the fraction of α-form modification X_α and the fraction of mesophase X_m (**Table 1**). On the basis of WAXS measurements the maximum total crystallinity was found for a low concentration of organoclays and, at the same time, the maximum draw ratio. Results are consistent with those obtained by the DSC-CLM method. With a higher concentration of C15A organoclay, the total crystallinity of the PP matrix gradually decreases, mainly due to a significant decrease in the mesophase fraction X_m. The higher content of α-modification was found for drawn fibres and a higher content of C15A organoclay. The sizes of α-form crystallites decrease gradually at a lower draw ratio and higher concentration of C15A organoclay in the PP matrix.

SAXS measurement was used for evaluation of d-spacing between silicate layers in the C15A and C30B organoclays (**Figures 4, 5**). Three characteristic intensity peaks were found for pure C15A organoclay corresponding to d-spacing of 3.5, 2.0 and 1.3 nm, respectively, and one peak for C30B organoclay corresponding to a distance of 1.9 nm between layers of the silicate. Only a single characteristic peak for C15A organoclay, corresponding to d = 2.0 nm, in the PP fibres appeared at a higher concentration (1 - 3 wt.%) and lower draw ratio (λ_1, λ_3). The peak for C15A in PP fibres is weak and broad. This could not be resolved for high draw ratio and lower concentration (0.02 - 0.1%), (**Figures 4.b, 5.a**). The results show that the cold drawing of fibres contributes to the intercalation and exfoliation of C15A organoclay in the matrix of PP fibres. The intercalated and exfoliated fraction of or-

ganoclay grows at a lower concentration of organoclay and high draw ratio.

The d-spacing of C30B in the PP fibres is clearly lower by 0.4 nm compared to pure C30B powder. Only for PP/C30B (1.0% + TEG) fibres at λ_{max} is the intensity peak slightly shifted towards smaller angles (larger distance) in comparison with composites without a TEG compatibiliser-dispersant. The intensity peaks of other samples remained in the same position (*Figure 5.b*); however, the difference is very minute. Based on SAXS results the d-spacing of C30B collapsed and the distance between layers decreased from 1.9 to 1.5 nm. The organic phase partially removes space from the layers in the PP matrix. This phenomenon is not rare for layered silicates and has also been presented in other papers.

The SAXS results show that the d-spacing of C15A organoclay in PP fibres grows during spinning and drawing mainly at a low concentration and maximum draw ratio. In contrast, no positive change regarding the intercalation and exfoliation of C30B organoclay was observed.

In the case of C15A organoclays, the higher amount of alkyl ammonium ion and higher compatibility of hybrid particles with PP enables the diffusion of polymer chains into galleries of silicates and, consequently, the forming of uniform composite morphology.

Sonic average orientation of fibres

Analysis of the average orientation f(α) carried out using the sonic velocity method shows the effect of organoclay on the orientation of structure elements in the PP matrix of PP/organoclay fibres (*Table 2*).

The positive effect of organoclay C15A and C30B was found at the maximum draw ratio (λ_{max}) and concentration of organoclays of about 0.1 wt.%. A higher content of organoclays leads to a decrease in the orientation of fibres at a constant draw ratio (λ_3) but also at the maximum draw ratio (λ_{max}). A higher average orientation was obtained for PP/C15A compared to PP/C30B fibres. Compatibiliser–dispersant S44P contributes to a higher orientation of PP/C15A fibres, and the TEG compatibiliser facilitates the orientation 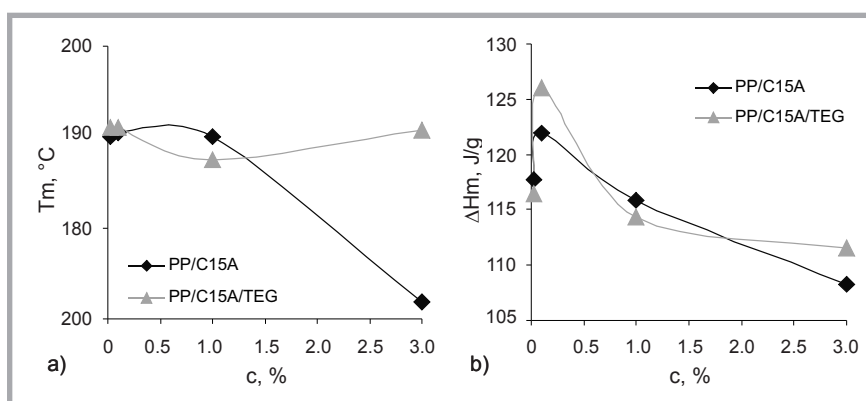of both PP/C15A and PP/C30B fibres. The results of the orientation of fibres correspond with those obtained by the DSC-CLM method and with the mechanical properties of fibres.

The effect of MMT at low concentration and the absence of a continuous phase of solid particles on the sonic velocity of composite fibres was considered as negligible.

Figure 4. SAXS curves for evaluation the d-spacing of pure organoclay (a) and PP/organoclay C15A 1.0 wt.% composite fibres (b). Slit-smeared data after Lorentz correction.
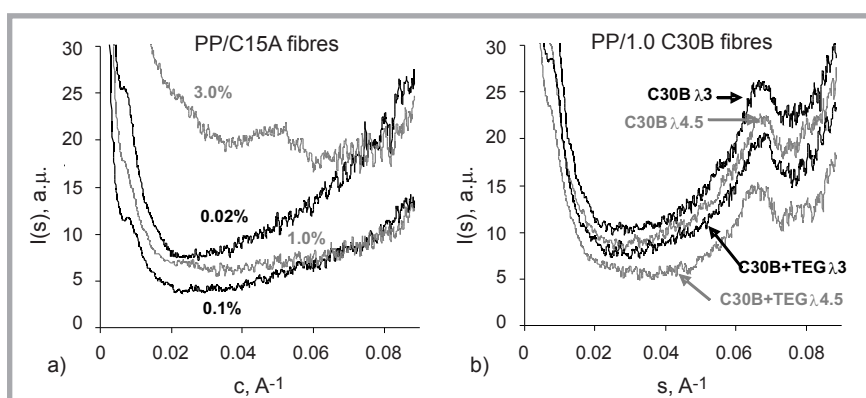

Figure 5. SAXS curves for evaluation the d-spacing of PP/organoclay composite fibres in dependence on concentration of C15A for λmax (a) and draw ratio of PP/C30B 1.0 wt.% fibres (b). Slit-smeared data after Lorentz correction.

Table 2. Average orientation f_α of the PP/C15A and PP/C30B drawn composite fibres (λ_3 and λ_{max}), the content of compatibiliser is 40 wt.% related to the organoclay content.

Composition of fibres	Content of organoclay, %	f_α of PP/C15A fibres		f_α of PP/C30B fibres	
		λ_3	λ_{max}	λ_3	λ_{max}
PP	-	0.64	0.72	0.64	0.72
PP/OC	0.02	0.64	0.76	0.62	0.74
	0.1	0.63	0.76	0.66	0.75
	1.0	0.62	0.70	0.61	0.73
	3.0	0.53	0.64	-	-
PP/OC/S44P	0.02	0.64	0.75	0.59	0.69
	0.1	0.63	0.76	0.64	0.75
	1.0	0.64	0.71	0.63	0.69
	3.0	0.61	0.70	0.34	0.54
PP/OC/TEG	0.02	0.64	0.76	0.63	0.74
	0.1	0.63	0.75	0.62	0.73
	1.0	0.62	0.72	0.64	0.72
	3.0	0.60	0.71	0.50	0.62

Mechanical properties

Both organoclays positively affect the tenacity and Young's modulus of PP composite fibres only at a low concentration,
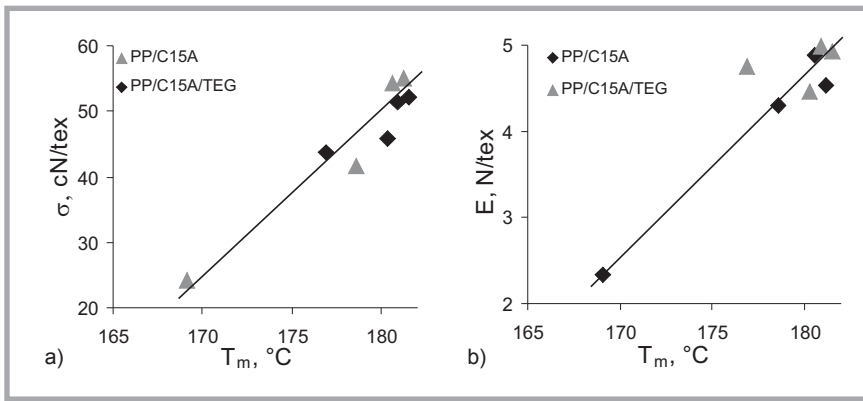
Figure 6. *Dependence of the tenacity σ versus melting temperature Tm (a) and Young's modulus E versus melting enthalpy ΔHm (b) (DSC-CLM) of PP/C15A composite fibres.*

Table 3. *Tensile strength σ, elongation at break ε and Young's modulus E of PP/C15A nanocomposite fibres.*

Fibres	C_{OC} in fibre, %	Draw ratio λ_{max}		
		σ, cN/tex	ε, %	E, N/tex
-	-	41.6 ± 0.7	33.8 ± 4.1	4.73 ± 0.17
PP/C15A	0.02	54.2 ± 3.5	27.7 ± 4.1	4.89 ± 0.25
	0.1	55.0 ± 1.9	25.6 ± 2.0	4.54 ± 0.42
	1.0	41.7 ± 2.4	36.1 ± 5.6	4.30 ± 0.28
	3.0	24.3 ± 0.8	98.5 ± 7.9	2.34 ± 0.08
PP/C15A/S44P	0.02	51.7 ± 2.9	27.2 ± 4.4	4.65 ± 0.30
	0.1	53.1 ± 1.0	26.0 ± 1.3	4.57 ± 0.26
	1.0	43.2 ± 1.8	34.2 ± 9.4	4.58 ± 0.24
	3.0	38.3 ± 2.0	41.0 ± 12.4	3.76 ± 0.16
PP/C15A/TEG	0.02	52.2 ± 1.9	25.3 ± 2.0	4.92 ± 0.16
	0.1	51.4 ± 1.3	24.1 ± 1.6	4.99 ± 0.11
	1.0	43.8 ± 1.4	44.7 ± 14.2	4.75 ± 0.23
	3.0	45.8 ± 2.9	25.8 ± 4.0	4.46 ± 0.17

Table 4. *Tensile strength σ, elongation at break ε and Young's modulus E of PP/C30B nanocomposite fibres.*

Fibres	C_{OC} in fibre, %	Draw ratio λ_{max}		
		σ, cN/tex	ε, %	E, N/tex
-	-	41.6 ± 0.7	33.8 ± 4.1	4.73 ± 0.17
PP/C30B	0.02	52.5 ± 1.9	29.4 ± 4.0	4.99 ± 0.19
	0.1	49.4 ± 2.3	27.2 ± 3.3	4.83 ± 0.16
	1.0	43.9 ± 1.6	20.3 ± 1.3	4.78 ± 0.18
	3.0	-	-	-
PP/C30B/S44P	0.02	44.4 ± 1.7	43.4 ± 11.9	4.56 ± 0.16
	0.1	56.7 ± 0.8	24.6 ± 1.7	5.38 ± 0.14
	1.0	38.1 ± 3.4	24.7 ± 6.2	4.57 ± 0.27
	3.0	12.3 ± 0.7	58.5 ± 13.3	1.49 ± 0.10
PP/C30B/TEG	0.02	56.3 ± 0.8	25.2 ± 1.0	5.31 ± 0.22
	0.1	55.1 ± 0.9	26.0 ± 1.4	4.73 ± 0.35
	1.0	44.0 ± 2.4	28.3 ± 3.2	4.68 ± 0.18
	3.0	22.4 ± 1.5	81.8 ± 11.2	2.25 ± 0.14

up to 1.0 wt% (***Tables 3, 4***). A lower tenacity was found for PP fibres containing C30B without a compatibiliser and with S44P .

Analysis of the mechanical properties of fibres shows the predominant effect of the supermolecular structure and orientation of fibres on both the tenacity and Young's modulus (***Tables 2 - 4, Figure 6***). The orientation of fibres results from their deformation in drawing. The positive effect of the low concentration of organoclay and compatibilisers on the mechanical properties of PP composite fibres resides in the favourable deformation during the drawing process. A

higher λ_{max} at the drawing of fibres was achieved in this case.

From the thermal properties of PP composite fibres, it can be concluded that while the melting temperature T_m obtained using the DSC-CM method for PP composite fibres increases slightly with the draw ratio, passing through the broad maximum, the T_m obtained by the DSC-CLM method grows proportionally with the draw ratio (***Figure 1.b, 2.a***). Analysis of these dependences and tensile properties of the composite fibres shows the proportionality between the tenacity of fibres and melting temperatures T_m (***Figure 6.a***). The highest T_m temperature corresponds to the highest tenacity and modulus of fibres at the maximum draw ratio λ_{max} within a 0.02 - 0.1 wt% concentration of organoclay in PP fibres.

The melting enthalpy ΔH_m obtained by the DSC-CLM method increases with the draw ratio of the fibres. The sharp maximum of the melting enthalpy at 0.02 - 0.1 wt% of C15A (***Figure 2.b***) clearly corresponds to the highest values of tensile properties of PP composite fibres (***Figure 6.b***).

With regard to the results obtained, the higher tensile properties of PP/organoclay composite fibres correspond to higher total crystallinity and a finer supermolecular structure, e.g. lower size of α-form crystallites. In addition, the lower content of mesophase crystallites has a positive effect on the tensile properties of fibres (***Tables 1, 3 & 4***). WAXS analysis of the PP composite fibres provides results corresponding to the DSC-CLM measurement. The higher tensile properties of PP composite fibres correspond to higher crystallinity (melting enthalpy), (***Table 1, Figures 3.b & 6.b***), orientation of the amorphous region – higher T_m (***Figure 6.a***), higher average orientation (***Table 2***), higher α-form fraction and lower size of both α-form and mesophase crystallites (***Table 1***).

■ **Conclusions**

The analysis of the thermal properties, supermolecular structure, orientation and mechanical properties of PP/organoclay composite fibres obtained in the experimental work allow to draw the following conclusions:

- The tenacity and Young's modulus of the PP/organoclay composite fibres correspond to their DSC-CLM melting temperature (orientation of non-crystalline regions) and melting enthalpy (total crystallinity). The higher melting the temperature T_m and melting enthalpy ΔH_m, the higher the tenacity and modulus of fibres.

- The tenacity and Young's modulus of PP/organoclay fibres increase gradually with a higher total crystallinity obtained by the WAXS method, a higher α-form fraction, a lower fraction of mesophase crystallites and with a lower size of both the α-form and mesophase crystallites. These parameters were found for PP/organoclay composite fibres containing 0.02 - 1.0 wt% of organoclay C15A (C30B with TEG dispersant only).

- The DSC-CLM method is suitable for the evaluation of thermal properties of drawn PP and PP/organoclay composite fibres. This method is more sensitive for oriented polymers in comparison with conventional DSC measurements. □

References

1. Wang K, Xiao Y, Na B, Tan H, Zhang Q, Fu Q. Shear amplification and re-crystallization of isotactic polypropylene from an oriented melt in presence of oriented clay platelets. *Polymer* 2005; 46(21): 9022-9032.

2. Ma J, Zhang S, Qi Z, Li G, Hu Y. Crystallization behaviors of polypropylene/montmorillonite nanocomposite. *J. App. Polym. Sci.* 2002; 83(9): 1978-1985.

3. Zhang QX, Yu ZZ, Yang M, Ma J, Mai YW. Multiple melting and crystallization of nylon-66/montmorillonite nanocomposites. *J. Polym. Sci. Part B: Polymer Physics* 2003; 41(22): 2861-2869.

4. Maiti P, Nam PH, Okamoto M, Hasegawa N, Usuki A. Influence of Crystallization on Intercalation, Morphology, and Mechanical Properties of Polypropylene/Clay Nanocomposites. *Macromolecules* 2002; 35(6): 2042-2049.

5. Somwangthanaroj A, Lee EC, Solomon MJ. Early Stage Quiescent and Flow-Induced Crystallization of Intercalated Polypropylene Nanocomposites by Time-Resolved Light Scattering. *Macromolecules* 2003; 36(7): 2333-2342.

6. Nowacki R, Monasse B, Piorkowska E, Galeski A, Handin JM. Spherulite nucleation in isotactic polypropylene based nanocomposites with montmorillonite under shear. *Polymer* 2004; 45(14): 4877-4892.

7. Choi WJ, Kim SCH. Effects of talc orientation and non-isothermal crystallization rate on crystal orientation of polypropylene in injection-molded polypropylene/ethylene–propylene rubber/talc blends. *Polymer* 2004; 45(7): 2393-2401.

8. Hambir S, Bulakh N, Jog JP. Polypropylene/Clay nanocomposites: Effect of compatibilizer on the thermal, crystallization and dynamic mechanical behaviour. *Polym. Eng. Sci.* 2002; 42(9): 1800-1807.

9. Peterlin A. Molecular model of drawing polyethylene and polypropylene. *J. Mater. Sci.* 1971; 6(6): 490-508.

10. Chatterjee A, Deopura BL. High modulus and high strength PP nanocomposite filament. *Composites, Part A.* 2006; 37(5): 813-817.

11. Tomio K, Seiichi M. Preparation of easily dyeable polyethylene terephthalate fibre. JP57161120, 1982.

12. Young RJ, Eichhorn SJ. Deformation mechanisms in polymer fibres and nanocomposites. *Polymer* 2007; 48(1): 2-18.

13. Young RJ. Monitoring Deformation Processes in High-performance Fibres using Raman Spectroscopy. *J. Text. Inst.* 1995; 86(2): 360-381.

14. Grebowicz JS, Brown H, Chuah H, Olvera JM, Wasiak A, Sajkiewicz P, Ziabicki A. Deformation of undrawn poly(trimethylene terephthalate) (PTT) fibres. *Polymer* 2001; 42(16): 7153-7160.

15. Lyon RE, Farris RJ, MacKnight WJ. A differential scanning calorimetry method for determining strain-induced crystallization in elastomeric fibres. *J. Polym. Sci. Polym. Lett. Ed.* 1983; 21(5): 323-328

16. Marcinčin A, Hricová M, Marcinčin K, Hoferíková A. Spinning of Polypropylene/Organoclay Composites, Thermal and Mechanical Properties of Fibres. *Tekstil: Časopis za tekstilnu techniku i konfekciju* 2008; 57(4): 141-148.

17. Marcinčin A, Hricová M, Marcinčin K, Hoferíková A. Study of Rheological, Thermal and Mechanical Properties of Polypropylene/Organoclay Composites and Fibres. *Fibres and Textiles in EE* 2009; 17(6): 22-28.

18. Rabiej M. Determination of the degree of crystallinity of semicrystalline polymers by means of the „OptiFit" komputer software. *Polimery* 2002; 47: 423.